



John, D. A., Parameswaran, C., Sandhu, S. and Dahiya, R. (2023) Silk nanofibers based soft and degradable capacitive pressure sensor arrays. *IEEE Sensors Letters*, 7(5), 2501104.



Copyright © 2023 IEEE. Reproduced under a [Creative Commons Attribution 4.0 International License](https://creativecommons.org/licenses/by/4.0/).

For the purpose of open access, the author(s) has applied a Creative Commons Attribution license to any Accepted Manuscript version arising.

<https://eprints.gla.ac.uk/297843/>

Deposited on: 4 May 2023

Enlighten – Research publications by members of the University of Glasgow  
<https://eprints.gla.ac.uk>

# Silk Nanofibers based Soft and Degradable Capacitive Pressure Sensor Arrays

Dina Anna John<sup>1</sup>, Chithra Parameswaran<sup>2</sup>, Sofia Sandhu<sup>1</sup>, and Ravinder Dahiya<sup>3\*</sup>

<sup>1</sup> James Watt School of Engineering, University of Glasgow, G12 8QQ, UK

<sup>2</sup> Department of Instrumentation and Applied Physics, Indian Institute of Science, 560012, India

<sup>3</sup> Bendable Electronics and Sustainable Technologies (BEST) group, Northeastern University, Boston, MA 02115, USA

\* Fellow, IEEE

**Abstract**— Highly sensitive pressure sensors with features such as biocompatibility, biodegradability, and flexibility are needed in applications such as robotics, prosthesis, medical implants, and wearable electronics. However, due to material limitations or technological bottlenecks it is often challenging to fabricate pressure sensors with these attributes at the same time. Herein, we present biodegradable silk/PEO/yeast nanofibers based soft capacitive pressure sensor array (2 × 2). The electrospun nanofibers used here have about 150% enhanced crystallinity, as confirmed by X-ray diffraction (XRD) and Fourier Transform- Infrared spectroscopy (FT-IR). The performance metrics of the sensor array, such as sensitivity (~0.18 kPa<sup>-1</sup>), hysteresis (<16%), minimum response (~0.8 s), and recovery time (~1 sec) show its suitability for application such as smart plasters used for accelerated wound healing. Further, the degradability studies confirm the quick degradation of sensors, which can also be potentially controlled with suitable packaging.

**Index Terms**—biodegradability, electrospinning, hysteresis, pressure mapping, pressure sensor, recovery time, response time, sensitivity.

## I. INTRODUCTION

Soft pressure sensors are important for numerous applications such as biomedical devices, robotics, and interactive systems etc. For example, as part of electronic skin (e-skin), the pressure sensors provide a measure of contact force, which is needed for haptic feedback-based action in robotics, prosthesis, and rehabilitation devices such as smart gloves [1-3]. Likewise, they are used in different types of wearable systems to monitor physiological parameters such as blood pressure or the pressure applied with compression bandage at a wound site or in implantable systems for cardiovascular or blood flow monitoring [4-6]. As a result, various types of pressure sensors based on different transduction mechanisms (e.g., piezoresistive [7-9], piezoelectric [10, 11], capacitive[12-14] etc.), have been explored.

Recently, the emerging requirements of several of the above applications have led to pressure sensors with flexible form factors so that they can conform to curvy surfaces [15-17]. Further, various health monitoring and implantable systems also require pressure sensors to be made of biocompatible, and biodegradable materials [18-21]. Such sensors can either be for single use or can be used for longer periods by controlling their degradability using suitable packaging. The single use sensor made from biodegradable materials could offer interesting solutions for medical applications, as besides ensuring the hygiene requirements they could also help address the rapidly growing challenges related to medical and electronic waste [22, 23]. Soft degradable pressure sensors employ materials that can be safely broken down by the body or the environment and are less harmful to the environment. However, such sensors normally offer modest sensitivity, and it can be challenging to maintain a stable signal over

extended periods [20, 24, 25]. A potential solution is to use polymeric nanofibers prepared using a simple, cost-effective, and solution processing-based electrospinning approach. The nanofibers provide numerous advantages, such as lightweight, low-cost, easy to prepare, excellent dielectric strength, higher porosity, and superior mechanical flexibility. In addition, electrospinning is compatible with the widely used biocompatible and biodegradable polymers such as silk, cellulose, chitosan, PVA, PVP, PLA etc. [26, 27]. Silk based pressure sensors use a methanol based treatment for enhancing the secondary structure for higher sensitivity. Here, we have implemented yeast autolysis based in-situ structure enhancement eliminating any further treatment of obtained silk fiber for pressure sensing.

Considering above background, we present here a biodegradable pressure sensor array utilizing electrospun silk/PEO/yeast nanofibers. The performance metrics of the sensor array, such as sensitivity (~0.18 kPa<sup>-1</sup>), hysteresis (<16%), response (<2.3 s), and recovery time (< 4 sec), are higher than those of state-of-the-art biodegradable pressure sensors, where the sensitivity is 0.08 kPa<sup>-1</sup>[25]/0.01887 kPa<sup>-1</sup>[26] and response/recovery time is ~3 s, showing its suitability for application such as smart plasters used for accelerated wound healing. This paper is organized as follows. Section II describes materials and methods used for the fabrication of 2x2 capacitive pressure sensors array. This is followed by the presentation of results in section III. Finally, the key outcomes are summarized in section IV.

## II. MATERIALS AND METHODS

### A. Materials

Bombyx silk yarn was purchased from M/S Bombyx silk yarns and textiles, J & K, India. Sodium Carbonate (Na<sub>2</sub>CO<sub>3</sub>, 98%), Polyethylene

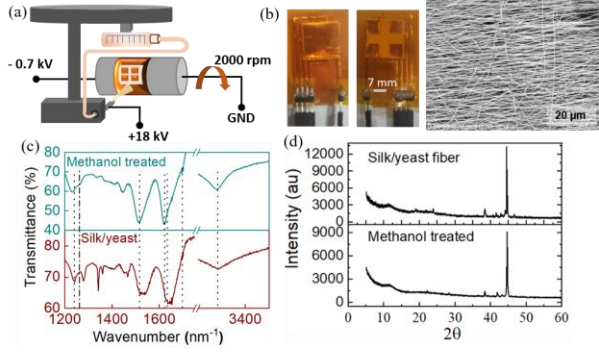


Fig. 1 (a) Fabrication of sensor array (b) Packaged sensor array (c) FTIR response and (d) XRD of silk fibers

Oxide (PEO, 9,000,000 Mv) and Lithium Bromide (Anhydrous, 99%) were purchased from Alfa Aesar Sigma Aldrich and Thermo Scientific, respectively. Slide – A-Lyzer® dialysis cassette (3,500 MWCO, 3-12 mL capacity); Slide – A-Lyzer™ Buoys were obtained from Thermo Scientific.

### B. Development of Nanofibers and fabrication of sensor array

As a first step, the array mask pattern was designed and patterned using Silhouette Cameo on thin PET sheet and attached to the patterned copper electrode. A  $2 \times 2$  copper electrode array pattern was created, with a single copper electrode (size -  $0.02 \times 0.02 \text{ m}^2$ ) serving as the bottom electrode and, four copper electrodes (size -  $0.007 \times 0.007 \text{ m}^2$ ) forming the top electrodes, thus making a simple structure. To prepare silk/yeast solution, 0.1 g of yeast was mixed with 1 mL of silk solution prepared by degumming in sodium carbonate solution followed by drying and combining with LiBr solution. Then, equal volumes of silk/yeast solution were blended with PEO and loaded to the syringe in the electrospinning machine. Fig. 1 (a) shows the electrospinning fabrication procedure for the sensor array and details can be seen in [28]. After electrospinning the silk/PEO/yeast on the electrodes, the final device was encapsulated in polyimide tape and electrical connection are attached for sensor characterisation.

### C. Sensor characterisation

Silk nanofibers were characterized using FE-SEM (Hitachi SU8230), FTIR (Nicolet Summit LITE, Thermo Fischer Scientific) and XRD (Miniflex, RIGAKU) to evaluate their morphological and compositional studies.

The fabricated sensor array was characterized using a LabVIEW controlled pressure generation setup, and the capacitance was measured using the Agilent 4284A, a precision LCR meter.

## III. RESULTS AND DISCUSSION

### A. Physico-chemical properties of silk/PEO/yeast nanofibers

The FTIR and XRD (Fig. 1 (c) and (d)) details the advantage of achieving ~ 150% enhancement in crystalline features. Table 1 elaborates upon the efficiency of the approach in terms of enhancing the crystallinity in silk fibers by comparing with typical methanol

Table 1. FTIR and XRD analysis showing enhancement in secondary structure in silk fibers.

Wavenumber (nm <sup>-1</sup> )	Methanol treated	Silk/yeast fiber	Enhancement %
1237	60.05	68.32	113.72
1261	63.3	71.5	112.95
1517	44.1	64.8	146.94
1622	43	63.6	147.91
1632	48	61.4	127.92
3283	61.1	72.7	118.98
2θ XRD intensity			
44.5	8970	13270	147.94
38.3	1392	2070	148.71
11.05	2338	3284	140.46

treated fibers i.e., the one without yeast. This crystallinity enhancement is distinctive feature of our work and it can help to develop sensors on large area, in a single step fabrication process.

### B. Performance metrics of the sensor array

The capacitance variation was recorded in the pressure range (0 – 390 kPa) by inputting an increasing pressure in steps for about 10 sec using a custom-made setup. The sensor response, i.e., capacitance change ratio ( $\frac{\Delta C_x}{C_{0x}}$  with  $\Delta C_x = C_x - C_{0x}$ , where  $C_x$ ,  $C_{0x}$  are the capacitances with and without pressure respectively, x represents the sensor number in the array) versus pressure during loading and unloading cycles is plotted in Fig. 2.

From the measurements, the hysteresis error can be calculated by the formula.

$$\text{Capacitance hysteresis \%} = \frac{\Delta C_x}{C_F C_{0x}} \times 100 \quad (1)$$

Where  $\frac{\Delta C_x}{C_{0x}}$  is the maximum capacitance change ratio and  $C_F$  is the full range of capacitance change ratio in a given cycle. The maximum capacitance hysteresis for all the sensors in the array was less than 16% as seen from Fig. 2.

Next performance metric is the sensitivity, for which the operating range of each sensor in the array is divided into three regions namely: Region I (0 to 4.56 kPa), Region II (4.56 to 44 kPa), and Region III (44 kPa to 390 kPa). The operating regions along with the equation relating the capacitance with the pressure are shown in Fig. 3. A higher

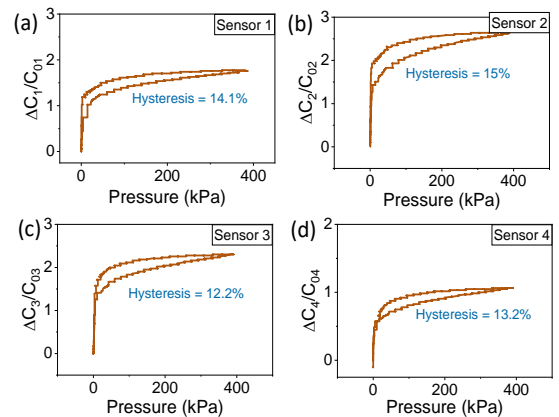


Fig. 2. Hysteresis graphs for each of the sensor in the array, (a) sensor 1, (b) sensor 2, (c) sensor 3 and (d) sensor 4.

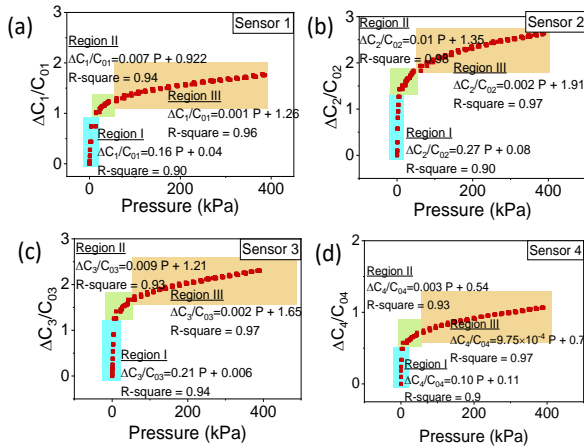


Fig. 3. Operating regions of the each of the sensor in the array and the equation relating to pressure, (a) sensor 1, (b) sensor 2, (c) sensor 3 and (d) sensor 4.

sensitivity of around  $0.18 \text{ kPa}^{-1}$  was observed in Region I due to the addition of air gaps in the silk/yeast nanofibers. When more pressure is applied, the air gaps reduce which literally stiffens the material due to hyperelasticity and increases the dielectric constant of the pressure sensor. This legitimately resulted in lower sensitivity in Regions II and III and an increase in the capacitance with pressure which is reflected in Fig. 3. The cause of hysteresis as well as the difference in the sensitivity values and other performance parameters for each sensor in the array is due to the electrospinning process, which cannot precisely control the size and location of the pores in the electrospun silk/yeast nanofiber, and the human errors involved while packaging the sensor array.

Due to the hyperelastic and porous nature of the silk/yeast nanofibers, the sensors were found to be relatively slower, with a response and recovery time of less than 4 s. As part of cyclic repeatability test, each of the four sensors were subjected to a pressure of 6.2 kPa for 20 cycles and the capacitance change ratio ( $\frac{\Delta C_x}{C_{0x}}$ ) of the sensors were found to be constant with a variation of ( $\pm 0.01$ ). These results are shown in Fig. 4. Hence, it can be stated that the sensor array is having high recovery properties. Some of the performance metrics of the sensor array has been calculated and is tabulated in Table 2.

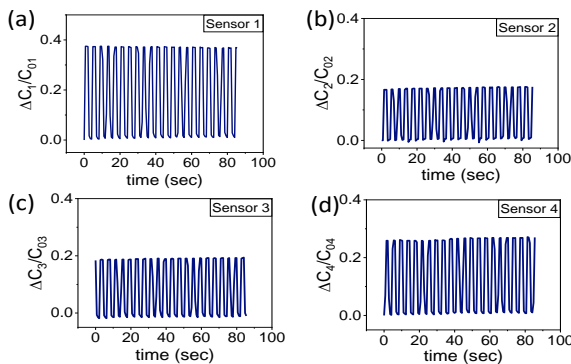


Fig. 4. Results from the cyclic repeatability test carried out for 20 cycles in the sensor array (a) sensor 1, (b) sensor 2, (c) sensor 3 and (d) sensor 4.

Table 2. Performance metrics of the capacitive sensor array.

Performance metrics	Values
Pressure range	0 – 390 kPa
Capacitance range	4 – 16 pF
Hysteresis	12 – 15 %
Response time	0.8 – 2.2 s
Recovery time	1 – 3.1 s
Sensitivity ( $\text{kPa}^{-1}$ )	$0.18 \pm 0.07$ for Region I (0 - 4.56 kPa) $0.007 \pm 0.003$ for Region II (4.56 – 44 kPa) $0.001 \pm 0.0005$ for Region III (44 – 390 kPa)

### C. Degradation studies

The degradation study of sensor was conducted in PBS buffer solution of pH = 4. The pH selection was based on initial studies carried out for each component of nanofibers based on their dissolution rate in acidic (pH=4) as well as basic buffers (pH=9). The results indicated that nanofibers dissolved more quickly in acidic medium than in basic medium. The solution containing SF/PEO/Yeast fiber-based device turned azure blue indicating the presence of  $\text{Cu}^{2+}$  ions on second day of the degradation period suggesting the interaction of copper with the ions present in buffer solution. Eventually, suspended particles started appearing in the solution indicating the detachment of fibers from the Cu tape. Polyimide on the other hand is non-biodegradable and hence is not interacting with any other ions. Complete dissolution of fibers and copper tape occurred after 120 days. In future, we will carry out the quantitative analysis of byproducts formed as a result of degradation.

### D. Application in pressure mapping

To demonstrate the application of the capacitive pressure sensor array, a touch map reconstruction was performed using PYTHON, which was interfaced with the Arduino. The schematic of the analog front-end for the electrospun capacitive pressure sensor array is shown in Fig. 5. The sensor ( $C_x$ ) is connected in series with a fixed capacitor ( $C_c$ ) and the voltage across  $C_c$  is fed to the analog pin of the Arduino. The square wave to the circuit is given by the Arduino. The Arduino collects the signals from the four sensors in the array using its analog pins. The Arduino code is written to display the pressure variation from the acquired voltage value, which changes with the capacitance of each of the sensor in the array. For this application, Arduino- Mega 2560 board is used.

When a change in external pressure is detected, the gradient variation in the pixel (each pixel represents a sensor in the array) within a window is generated by running the program in PYTHON. This is demonstrated in Fig.6. Here, the pressure in the display is limited to 100 kPa to distinguish between low and high pressure.

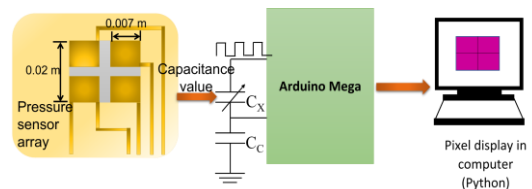


Fig. 5. Schematic of the pressure mapping application using electrospun pressure sensor array



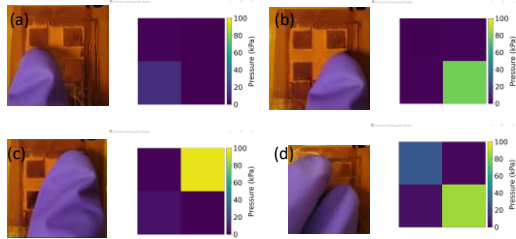


Fig.6. Pressure mapping demonstration w.r.t the different points of pressure, (a) pressing sensor 1, (b) pressing sensor 2, (c) pressing sensor 3 and (d) pressing sensor 2 and 4.

Hence, this application evidences the utility of the pressure sensor array in detecting the external pressure and the position of the pressure point.

#### IV. CONCLUSION

In summary, a  $2 \times 2$  pressure sensor array developed by electrospinning method is discussed in this paper. The pressure sensors array shows a sensitivity of  $0.18 \text{ kPa}^{-1}$  in the pressure region  $< 4.56 \text{ kPa}$ , low response and recovery time, low hysteresis ( $< 16\%$ ). They can be made environment friendly by single stage fabrication process. It was found that the materials used in the fabrication of the simple sensor array design presented in this paper are degradable with time (in about 120 days). Finally, the application of the sensor array in the pressure mapping has been carried out to identify the pressure point and the magnitude of external pressure applied. As a future work, the pressure sensor array discussed in this paper will be fabricated to form a large sensor array which can be interfaced with a wireless read-out system and attached to bandages for real time monitoring of external pressure on the wounds. We will also conduct further studies on biodegradability to understand the by-products of this process.

#### ACKNOWLEDGMENT

The work in this letter was initiated by R. Dahiya's Bendable Electronics and Sensing Technologies (BEST) Group when he was at the University of Glasgow, U.K. The work was completed after he moved to Northeastern University, USA, where his group is known as Bendable Electronics and Sustainable Technologies (BEST) Group. This work was supported in part by the European Commission through the FET-OPEN project Ph-Coding (H2020-FETOPEN-2018- 8291), Heteroprint Programme Grant (EP/R03480X/1) and CHIST-ERA project TESLA (EP/W035790/1).

#### REFERENCES

- [1] O. Ozioko and R. Dahiya, "Smart Tactile Gloves for Haptic Interaction, Communication, and Rehabilitation," *Advanced Intelligent Systems* vol. 4, pp. 1-22, 2022.
- [2] A. Paul, N. Yogeswaran, and R. Dahiya, "Ultra-Flexible Biodegradable Pressure Sensitive Field Effect Transistors for Hands-Free Control of Robot Movements," *Adv Intelligent Sys*, vol. 4, pp. 1-16, 2022.
- [3] O. Ozioko, P. Karipoth, P. Escobedo, M. Ntagios, A. Pullanchiyodan, and R. Dahiya, "SensAct: The Soft and Squishy Tactile Sensor with Integrated Flexible Actuator," *Adv Intelligent Sys*, vol. 3, pp. 1-12, 2021.
- [4] F. Nikbakhtnasrabadi, E. S. Hosseini, S. Dervin, D. Shakthivel, and R. Dahiya, "Smart Bandage with Inductor-Capacitor Resonant Tank Based Printed Wireless Pressure Sensor on Electrospun Poly-L-Lactide Nanofibers," *Adv Electron Mater*, vol. 8, pp. 1-11, 2022.
- [5] Y. Park *et al.*, "Wireless, skin-interfaced sensors for compression therapy," *Science Advances*, vol. 6, no. 49, p. 1655, 2020.
- [6] C. M. Boutry *et al.*, "A Stretchable and Biodegradable Strain and Pressure Sensor for Orthopaedic Application.," *Nature Electronics*, vol. 1, pp. 314-321, 2018.

- [7] P. Karipoth, A. Pullanchiyodan, A. Christou, and R. Dahiya, "Graphite-Based Bioinspired Piezoresistive Soft Strain Sensors with Performance Optimized for Low Strain Values," *Acs Appl Mater Inter*, vol. 13, no. 51, pp. 61610-61619, 2021.
- [8] S. J. Park, J. Kim, M. Chu, and M. Khine, "Flexible Piezoresistive Pressure Sensor Using Wrinkled Carbon Nanotube Thin Films for Human Physiological Signals," *Advanced Materials Technologies*, vol. 3, pp. 1-7, 2017.
- [9] M. Bhattacharjee, M. Soni, P. Escobedo, and R. Dahiya, "PEDOT: PSS microchannel based highly sensitive stretchable strain sensor," *Advanced Electron Mater*, vol. 6, pp. 1-9, 2020.
- [10] N. Yogeswaran, E. S. Hosseini, and R. Dahiya, "Graphene Based Low Voltage Field Effect Transistor Coupled with Biodegradable Piezoelectric Material Based Dynamic Pressure Sensor," *Acs Appl Mater Inter*, vol. 12, no. 48, pp. 54035-54040, 2020.
- [11] S. Ma, Y. Kumaresan, A. S. Dahiya, L. Lorenzelli, and R. Dahiya, "Flexible Tactile Sensors using AlN and MOSFETs based Ultra-thin Chips," *Ieee Sens J*, p. 1, 2022.
- [12] Y. Kumaresan, S. Ma, O. Ozioko, and R. Dahiya, "Soft Capacitive Pressure Sensor With Enhanced Sensitivity Assisted by ZnO NW Interlayers and Airgap," *Ieee Sens J*, vol. 22, no. 5, pp. 3974-3982, 2022.
- [13] E. S. Hosseini, M. Chakraborty, J. Roe, Y. Petillot, and R. Dahiya, "Porous Elastomer Based Wide Range Flexible Pressure Sensor for Autonomous Underwater Vehicles," *Ieee Sens J*, vol. 22, no. 10, pp. 9914-9921, 2022.
- [14] O. Ozioko, W. Navaraj, M. Hersh, and R. Dahiya, "Tacsac: A Wearable Haptic Device with Capacitive Touch-Sensing Capability for Tactile Display," *Sensors-Basel*, vol. 20, no. 17, pp. 1-15, 2020.
- [15] S. Lee *et al.*, "A transparent bending-insensitive pressure sensor," *Nature nanotechnology*, vol. 11, no. 5, pp. 472-478, 2016.
- [16] F. Nikbakhtnasrabadi, H. El Matbouly, M. Ntagios, and R. Dahiya, "Textile based stretchable microstrip antenna with intrinsic strain sensing," *ACS Appl. Electron. Mater.*, vol. 3, no. 5, pp. 2233-2246, 2021.
- [17] F. Liu, S. Deswal, A. Christou, Y. Sandamirskaya, M. Kaboli, and R. Dahiya, "Neuro-inspired electronic skin for robots," *Science robotics*, vol. 7, no. 67, pp. 17344, 2022.
- [18] E. S. Hosseini, S. Dervin, P. Ganguly, and R. Dahiya, "Biodegradable Materials for Sustainable Health Monitoring Devices," *ACS applied bio materials*, vol. 4, no. 1, p. 163, 2021.
- [19] G. Khandelwal, G. Min, X. Karagiorgis, and R. Dahiya, "Aligned PLLA Electrospun Nanofibers based Biodegradable Triboelectric Nanogenerator," *Nano Energy*, vol. 110, 2023.
- [20] Y. Jiang *et al.*, "Wireless, closed-loop, smart bandage with integrated sensors and stimulators for advanced wound care and accelerated healing," *Nat Biotechnol*, 2022.
- [21] Y. K. Shin, Y. Shin, J. W. Lee, and M. H. Seo, "Micro-/Nano-Structured Biodegradable Pressure Sensors for Biomedical Applications," *Biosensors (Basel)*, vol. 12, no. 11, 2022.
- [22] M. Chakraborty, J. Kettle, and R. Dahiya, "Electronic Waste Reduction Through Devices and Printed Circuit Boards Designed for Circularity," *IEEE Journal on Flexible Electronics*, vol. 1, no. 1, pp. 4-23, 2022.
- [23] A. Beniwal, D. A. John, and R. Dahiya, "PEDOT:PSS based disposable humidity sensor for skin moisture monitoring," *IEEE Sensor Letters*, vol. 7, no. 3, p.1, 2023.
- [24] J. Park, J. K. Kim, S. J. Patil, J. K. Park, S. Park, and D. W. Lee, "A Wireless Pressure Sensor Integrated with a Biodegradable Polymer Stent for Biomedical Applications," *Sensors (Basel)*, vol. 16, no. 6, 2016.
- [25] A. Elsayes, V. Sharma, K. Yiannacou, A. Koivikko, A. Rasheed, and V. Sariola, "Plant-Based Biodegradable Capacitive Tactile Pressure Sensor Using Flexible and Transparent Leaf Skeletons as Electrodes and Flower Petal as Dielectric Layer," *Advanced Sustainable systems*, vol. 4, 2020.
- [26] C. Hou *et al.*, "A Biodegradable and Stretchable Protein - Based Sensor as Artificial Electronic Skin for Human Motion Detection," vol. 15, no. 11, p. 1805084, 2019.
- [27] M. A. Kafi, A. Paul, A. Vilouras, and R. Dahiya, "Mesoporous chitosan based conformable and resorbable biostrip for dopamine detection," *Biosensors & bioelectronics*, vol. 147, pp. 111781-111781, 2020.
- [28] C. Parameswaran, D. Shakthivel, and R. Dahiya, "Fabrication of silk nanofibers with in-situ crystallization for large- area tactile sensing," presented at the IEEE Applied Sensing Conference (APSCON), Bengaluru, Jan 2023.